Undergraduate Honors Theses   Student Works

5-2023

Synthesis of a Phenyl Substituted Zinc Dipyrrin Complex for the Purpose of Analyzing Aromatic Substitutions on the Characteristics of Compounds of this Class

Kole Owen

Follow this and additional works at: https://dc.etsu.edu/honors

Part of the Analytical Chemistry Commons, Environmental Chemistry Commons, Inorganic Chemistry Commons, Oil, Gas, and Energy Commons, Organic Chemistry Commons, and the Sustainability Commons

Synthesis of a Phenyl Substituted Zinc Dipyrrin Complex for the Purpose of Analyzing

Aromatic Substitutions on the Characteristics of Compounds of this Class

by

Kole Owen

An Undergraduate Thesis Submitted in Partial Fulfillment
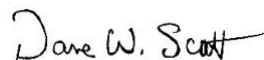
of the Requirements for the University Honors Program

East Tennessee State University

_____

Kole Owen

_____

Dr. Catherine McCusker, Thesis Mentor

_____

Dr. Dane Scott, Reader

Abstract

The field of photochemistry is as innovative in development as it is broad in application. However, utilization of energy from the sun's electromagnetic radiation remains secondary to the combustion of fossil fuels for the global energy consumption. This is neither a sustainable nor renewable system, and it has contributed to a major decline in the health of our global environment as the greenhouse gases emission has led to an incline in global temperatures and ocean acidity. To develop effective ways to utilize solar energy, experimental effort is being directed towards the understanding of photosensitizers, molecules which absorb solar radiation and initiate redox chemistry in CO_2 reduction catalysts. Some zinc dipyrrins, one such class of photosensitizers, are theorized to undergo intersystem crossing through a charge separated state, a transition that is stabilized in polar solvents. This transition increases the lifetime of the excited state, as relaxation from the triplet state occurs much slower than from the singlet state. A phenyl substituted zinc dipyrrin was attempted to be synthesized and characterized using NMR spectroscopy to probe aromatic substituent effects on the molecule's photophysics. The product was analyzed by UV-vis spectroscopy in order to confirm its purity and TLC analysis shows that the reaction kinetics are much slower in this phenyl substituted zinc dipyrrin than in previous reports, most likely due to the steric hindrance induced by the bulky phenyl substitutions.

<u>Acknowledgements</u>

First and foremost, glory goes to the Creator. He has made a good work, a wonderfully complex world, and it is my honor and privilege to study it and so get to know Him through it.

Next, thanks go to Dr. McCusker. She has been a great and ready help to me throughout this process. She is a professor I can say cares as much about her students as she does her research. Her gracious help has been invaluable in the progression of my knowledge and skills in chemistry. I would like to thank my reader, Dr. Scott, as his feedback and criticism allowed me to put forth my best possible work. And thank you, the one who reads this now. Your interest in my work helps realize my dream of pursuing chemistry and the natural sciences as a career as well as a passion.

My utmost respect and gratitude go to my wife, Abby. She has offered a constant companionship throughout most of this process. She keeps the love and desire for learning alive inside of me. Last but certainly not least, a large thanks to my family and friends. They all, in some way, shape, or form, have carried me along to this culmination of my undergraduate experience.

<u>Contents</u>

List of Tables:

List of Figures

List of Abbreviations

Zinc Dipyrrin (ZnDIPY)

Charge Seperated (CS)

Inter System Crossing (ISC)

Inter Ligand Electron Transfer (ILET)

Boron Dipyrrin (BODIPY)

Nuclear Magnetic Resonance (NMR)

Ultraviolet-Visible (UV-vis)

Methanol (MeOH)

Triethyl amine (TEA)

Trifluoroacetic acid (TFA)

2,3-Dichloro-5,6-dicyano-1,4-benzoquinone (DDQ)

Dichloromethane (DCM)

Thin Layer Chromatography (TLC)

Phenyl (Ph)

Mesityl (Mes)

Chapter 1: Background

The Energy Issue and its Current State:

Hydrocarbon combustion has seen a dramatic rise in the global greenhouse gas emissions since the rise of the industrial revolution[1]. This has been linked to trends towards global warming[2] and ocean acidification[3], which may have dire effects on our planet's environments. Technology is rising to the challenge of reducing emissions. For example, electric vehicles are suggested to offset the combustion of fossil-fuel-based gasoline in engines. Criticism of electric vehicles includes varying real-world emissions based on the fuel source that drives electricity generation, which may be higher than that of a conventional internal combustion engine if based on coal[4]. Proposed solutions include the advancement of renewable energy systems like solar, wind, hydroelectric, and geothermal; however, the batteries required to store this energy may decrease their validity due to deficient energy storage densities[5,6].

Additionally, current infrastructure supports consumption of carbon-based fuel sources with 77% of energy directed to transportation, electricity production, and other industries sourced from natural gas, petroleum, and coal (Figure 1)[7]. Studies also show that as early as 1965, 80% of organic products were synthesized from petroleum, a number that jumped to 99% in 2000[8]. As of 2018, the petrochemical industry accounts for 12% of oil consumption and is estimated to account for 30% by 2030[9]. Predictions show an expected 83 billion cubic meters of natural gas annually and 7 million barrels of oil added to daily consumption within the petrochemical industry by 2050[9]. Furthering this issue, the fossil fuel extraction industry is not without environmental impact[8].
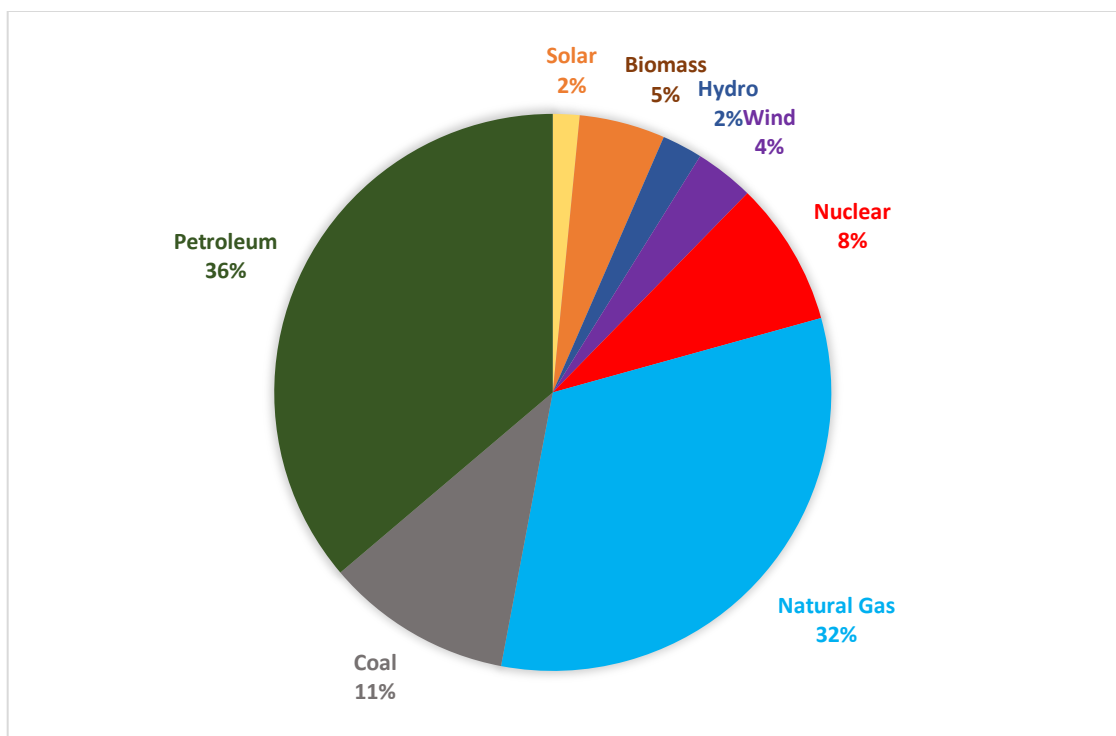
Figure 1: The United States 2021 energy consumption by source in percentage[7]

There requires a solution that satisfies the needs of a national and global economy and the health of a national and global environment. Enter artificial photosynthesis. This process, modelled off the natural manufacturing of sugars by plant-life and microorganisms, allows the synthesis of combustible hydrocarbons using carbon dioxide, sunlight, and a system of compounds that facilitate the reduction of CO_2 to more reactive products[5]. It has not escaped notice that this system may be an efficient and regulated method of carbon sequestering for the purpose of atmospheric carbon dioxide concentration modulation.

This system requires a catalyst with potentials suitable for the reduction, an electron donor which supplies the electron necessary for the carbon dioxide reduction, and a photosensitizer that harnesses solar energy in an excited state to receive an electron from the donor. In a reductive quenching pathway, the sensitizer acts as a

reducing agent, providing an electron to the catalyst (Figure 2)[10]. When practically

realized, the system would be able to produce carbon building blocks that may be easily

converted into fuels compatible with current infrastructure and many other valuable

organic compounds while attaining net carbon neutrality.
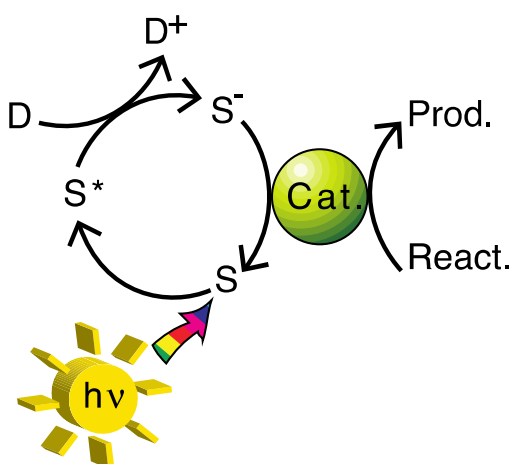
Figure 2: The reductive quenching pathway of a photocatalytic system. In this case, the photosensitizer (labelled 'S') is first excited by incident photons, then receives an electron from a sacrificial donor ('D') and delivers it to the catalyst to carry out its chemistry. The sensitizer is oxidized to its original state and can be excited again to repeat the cycle[10].

Research in this field is directed mainly towards the the catalyst[11–16] and the

photosensitizer[10,15–28]. The ideal system is one in which the components are maximally

compatible and efficient, are cheaply made and/or highly durable, and operate on

industrial scales in industrial setting. The McCusker Lab currently directs its attention

to the photosensitizer.
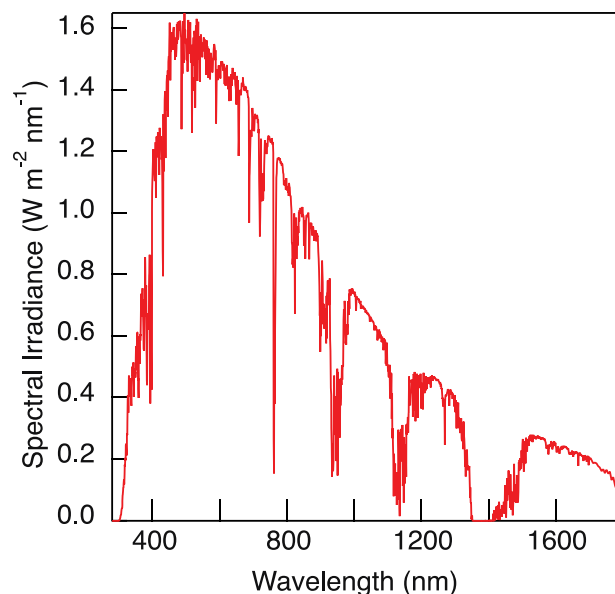
Figure 3: The AM1.5 solar spectrum, showing the spectral intensity by wavelength of light incident on the earth's surface[29].

A useful photosensitizer must meet the following criteria: 1) absorption of light in the solar spectrum, which is principally comprised of visible and near IR wavelengths (Figure 3)[29], 2) synthetic accessibility and/or high durability as a matter of course if to be used at industrial scale, and 3) and ability to maintain absorbed solar energy in an excited state long enough for the desired chemistry to ensue. For this research, the excited state lifetime is suitable if it falls in the microsecond timescale, as this is the threshold duration required for an excited photosensitizer to undergo successful interaction with the sacrificial electron donor. This threshold is determined based on the rate of diffusion of the molecule in the solvent and on reasonable concentrations of solute, which are dependent on its solubility and its cost.
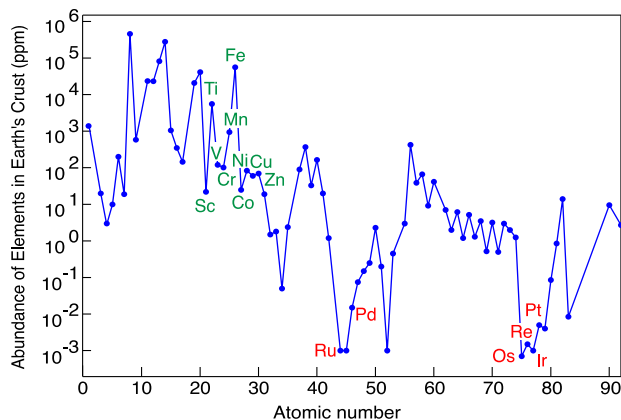
Figure 4: Abundance of naturally occurring elements in the Earth's crust with atomic numbers 1 through 92, except Tc[30].

Previous research shows there are photosensitizers that facilitate the photosynthetic mechanism but are not industrially viable. For instance, tris(2,2′-bipyridine)ruthenium(II) complexes[12,31] and tris(2-phenylpyrridine)iridium(III) complexes[14,31] are commonly applied as photosensitizers, along with many of their derivatives[12]. Use of organometallic compounds coordinated to second and third period transition metals like tungsten[31], tellurium[16], gold[11,32], and platinum[33] have also been reported. However, an inherent flaw with these central metals is their lack of abundance in the earth's crust[30] (Figure 4). Low abundance naturally results in high cost and negates the goal of a long-term solution as industrial scale use of these photosensitizers threatens to quickly exhaust supplies of these precious metals.

Other photosensitizers coordinated about first period transition metals, those of $3d^n$ electron configuration have shown promise but not viability. This principally has to do with the presence of ligand field states, which are the d-to-d electron transitions present in molecular orbital theory. For first period transition metals, these transitions are of lower energy than the charge transfer state transitions, as the crystal field splitting energy is relatively weak[34]. Relaxation from these states following excitation occurs very

quickly, decreasing the lifetime of the excited state[35]. The second and third period transition metals have a much greater crystal field splitting energy, which lends to a destabilization of the ligand field states[34]. As such relaxation occurs from the higher energy charge transfer states, which results in a longer lifetime of the excited state[34–36]. Transition metals of d^0 and d^{10} electron configurations disregard ligand field states, as there is no ability for electron transitions to occur between d orbitals[36].

Zinc Dipyrrins

Zinc Dipyrrins (ZnDIPY) are compounds in which two bidentate dipyrromethene ligands, typically of homoleptic identity, are coordinated to a zinc(II) central atom. Zinc acetate, the starting material for coordination of zinc to the dipyrrin, is largely available at ~ $1.40 per gram[37]. This is compared to ruthenium trichloride, the starting material for ruthenium coordination, at ~$60 per gram[38], and iridium trichloride at $520 per gram[39]. These prices reflect the abundance of the central metals, and it may be inferred that given similar yields in synthesis a zinc-centered photosensitizer would be much for cost efficient. Zn^{2+} has an electron configuration of [Ar] $3d^{10}$, making these metal centers redox inactive (Figure 5) and ameliorating the swift nonradiative decay from ligand field states[17,36].
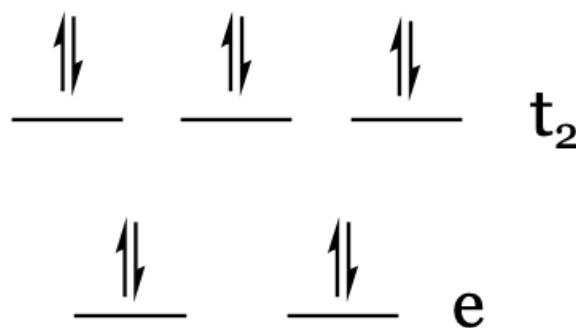
Figure 5: The crystal field diagram of a $3d^{10}$ electron configuration in a tetrahedral geometry[40,41].

Additionally, the electron geometry about the zinc center imposes a tetrahedral molecular geometry and orthogonal positioning of the ligands[17]. Orthogonal positioning is of great importance, since this typically results in very poor overlap between ligand orbitals, meaning the ligands would undergo very little electronic resonance with one another. As is discussed later, this facilitates the formation of the charge separated state that is theorized to promote intersystem crossing to the long-lived triplet state[17].

The dipyrromethene ligand, also known as a dipyrrin, is an oligopyrrole linked by a methylene bridge forming a conjugated π system. These ligands have been shown to absorb in the visible spectrum[20]. Additionally, the dipyrromethene ligand (Figure 6) may take on substitutions at all C-H bonds in the structure, allowing a degree of tuning to be done on the compound as the introduction of alkyl, aromatic, or heavy atom groups may alter the photophysics and photochemistry of the compound[24].
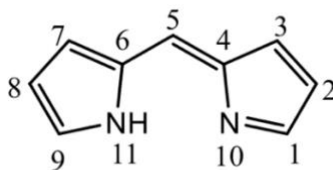
Figure 6: IUPAC numeric ordering for a dipyrromethene ligand. See that positions 4 and 6 are relatively inactive as they are electronically satisfied tertiary carbons[19].

Why is the orthogonal nature of a ZnDIPYs ligands of any importance?

Working theory presents the formation of a charge separated (CS) state between said ligands in polar solvents, which may provide a medium by which intersystem crossing (ISC) occurs after the molecule undergoes excitation[17,23,25]. The orthogonality of homoleptic ligands allows a symmetry breaking charge transfer whereby, upon excitation, an electron is transferred from one ligand to the other, enforcing a separated charge between the ligands. Polar solvents, which stabilize this CS state via

intermolecular interactions that generate a secondary coordination sphere[42], provide a state of intermediate energy by which ISC is facilitated (Figure 7). ISC is the spin-forbidden transition of an excited electron from a between two states, in this case between the singlet and triplet states[43]. This is an important attribute to a photosensitizer as the relaxation of energy from the triplet state radiatively by phosphorescence or non-radiatively by internal conversion, occurs much more slowly than relaxation from the singlet excited state back to the ground state either radiatively by fluorescence or non-radiatively[43]. This results in a molecule with an increased excited state lifetime. Coincidentally, CO_2 reductions are optimized by polar environments[44], providing further advantage to confirming and utilizing the CS state as a pathway to increase the probability ISC.
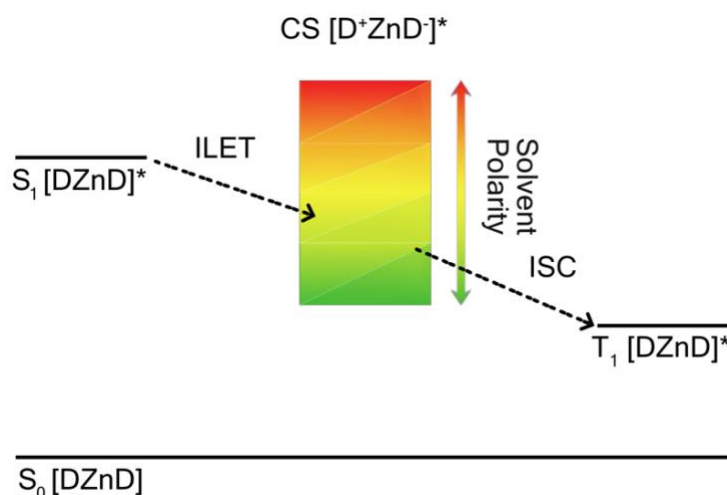
Figure 7: Qualitative Jablonski diagram showing the theorized effect of solvent polarity on the stability of the CS state. Inter-ligand electron transfer (ILET) results in a full charge separation rather in polar solvents [17].

These ZnDIPYs ride the coattails of the largely studied and famous compound of the photoluminescence world: the boron dipyrrin (BODIPY). These molecules have wide application in medicine as ion indicators and biomarkers in fluorescence microscopy[45,46], in industry as dyes in solar cells and lasers[47,48], and, related to this

research, as generally high efficiency fluorophores. BODIPYs (Figure 8) also utilize the

dypirrin ligand and so are structurally analogous to ZnDIPYs. They have been previously

characterized in many shapes and sizes[49,50], which may help motivate the substitutions

employed on ZnDIPYs that are under current design for photosensitization. Since the

BODIPY can only coordinate to one ligand, it does not form a CS state, making these

compounds incredible useful for understanding the change in photophysical properties

brought on by the CS state. These kinds of experiments control for the symmetric and

orthogonal nature of a homoleptic ZnDIPY and may confirm the CS state as the vehicle

by which ISC occurs.
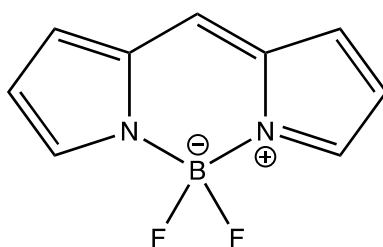
Figure 8: The skeleton structure of a BODIPY[49].

Previous Work

The McCusker lab has precedent to this research and have undergone

investigation of alkyl and heavy atom substituent effects on ZnDIPY characteristics

(Figure 9). As predicted in BODIPY predecessors, The successive addition of more alkyl

substituents generally resulted in a bathochromic shift in the absorption and emission

maxima[17,19,49]. In the strictly alkylated complexes, the fluorescence quantum yield was

indirectly related to the polarity of the solvent in which the measurements were taken,

indicating an alternate route of excited state decay. Transient absorption measurements

revealed an increase in the triplet state yield of the compounds proportional to the

solvent polarity in compound 1. It was this finding that motivated the symmetry breaking charge separation intermediate state theory of excited state decay[23,25].

The addition of the heavy iodine substituents in at positions 2 and 8 in compound 3 resulted in a large increase in triplet state yield as compared to compound 1 regardless of the polarity of the solvent in which the measurements were taken[10,17], indicating a relaxation pathway other than through a charge separated state intermediate for this complex. A presumable explanation is that the rate of intersystem crossing is dictated by the increase of spin-orbit coupling and vibrational overlap afforded by heavy atom substituents.

1   2   3
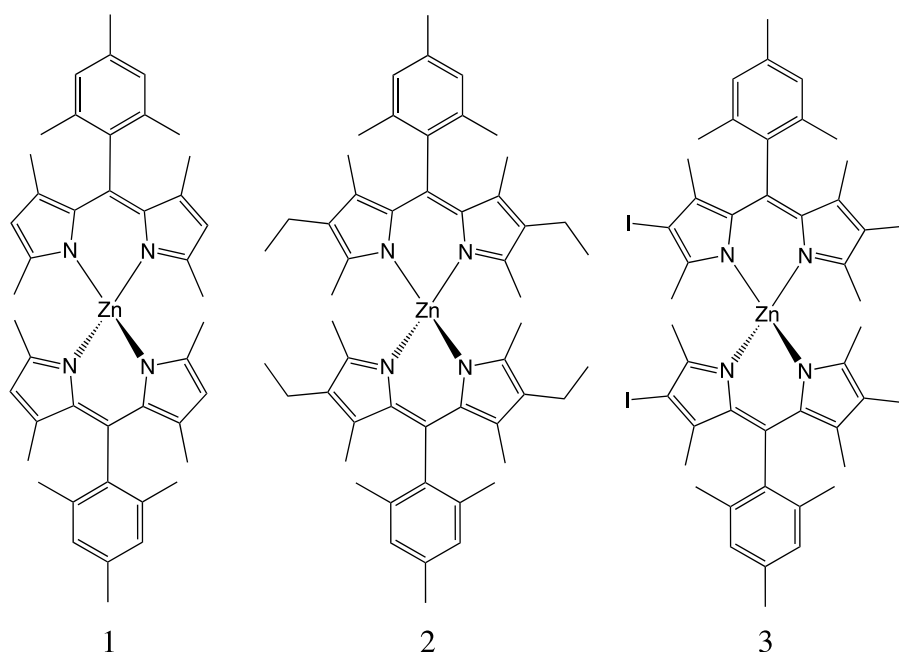
Figure 9: The structures of *bis*(1,3,7,9-tetramethyl-5-mesityldipyrronato)zinc(II), compound 1, and *bis*(2,8-diethyl-1,3,7,9-tetramethyl-5-mesityldipyrronato)zinc(II), compound 2, which probe alkyl substituent effects[10,17,19]. Compound 3, *bis*(2,8-diiodo-1,3,7,9-tetramethyl -5-mesityldipyrronato)zinc(II), probes the effect of heavy ion substitutions[10,17].

Research Aims:

Specific to this research, a *bis*(1,3,7,9-tetraphenyl-5-mesityldipyrronato) zinc(II) compound was attempted to be synthesized (Figure 10). The mesityl is included as the

electron density present on the methyl groups of the mesityl provide a steric hindrance, which restricts the conformational rotation of the group. As shown in previous research by Lindsey and coworkers, this reduces the amount of energy lost by non-radiative deactivation and increases excited state lifetime[24,28]. The phenyl groups probe the effect of aromatic substituents on the dipyrrin scaffold have on the characteristics of a ZnDIPY.

We hypothesize that the presence of the phenyl rings will increase the value of the extinction coefficient, which is the intensity of absorption, and the wavelength of maximum absorption as compared to an aryl-substituted analogs (e.g. compounds 1 and 2) by the expansion of the coordinated π-system. Both claims have precedent in the behavior of π-system expanded BODIPYs[49]. Previous research on ZnDIPY synthesis shows total yields between 5% and 13% using literature methods[10,19,25]. Two methods were explored to probe the yield of this compound's synthesis.
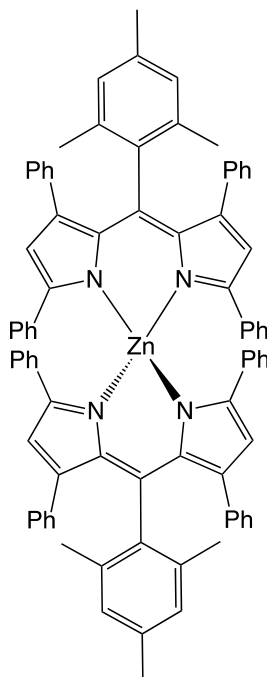
Figure 10: The structure of compound *bis*(1,3,7,9-tetraphenyl-5-mesityldipyrronato) zinc(II).

The synthesis of 1,3,7,9-tetraphenyl-5-mesityl-dipyrromethene was previously attempted by Meredith, followed by a purification of the ligand via alumina column chromatography before coordination to zinc (Figure 11)[18]. The uncoordinated nitrogen atoms of the ligand interact strongly with the alumina, which retarded the movement of the ligand through the column and disallowed successful purification[18]. In this synthesis, coordination to zinc will be attempted prior to purification in hopes that the zinc preferentially coordinates to the ligand, at which point the nitrogen is no longer exposed and the product should elute readily.
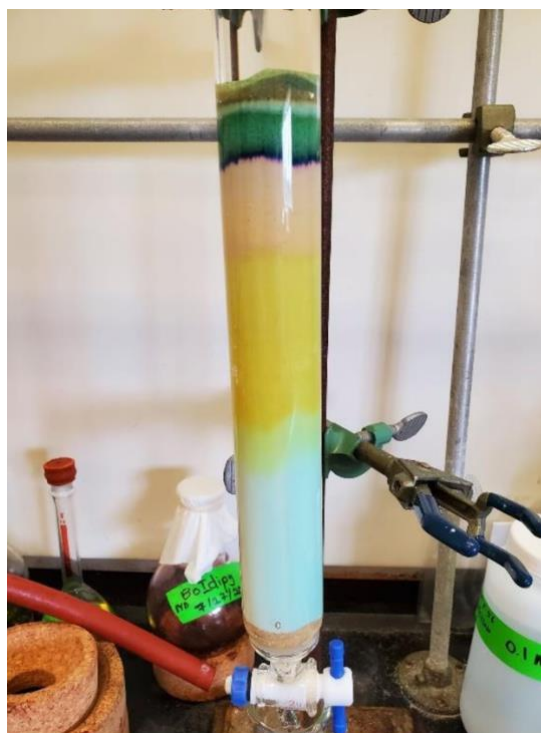
Figure 11: The purification of 1,3,7,9-tetraphenyl-5-mesityldiprromethene via alumina column chromatography[18]

Chapter 2: Experimental Methods

Unless methodology is accompanied by a specific source, the steps taken in synthesis and purification originated from various published sources[51,52] or online forums[53]. NMR data was collected using a 400 MHz JEOL AS400 FT-NMR spectrometer and analyzed using the SpinWorks 4.2.10 and iNMR softwares. UV-Vis absorption data was collected using the VWR UV6300PC double beam spectrophotometer. The reagents used originated from Fischer Scientific, except the 2,4-diphenyl-1H-pyrrole, which was purchased from Sigma Aldrich. Unless specified, reagents were used without prior purification.

Synthesis A

Figure 12: The synthesis A reaction scheme.

Attempt 1:

Synthesis of 1,3,7,9-tetraphenyl-5-mesityldyrromethene:

This synthesis step was based on the method described by Rogers (1943)[54]. To a flask, 2,4-diphenyl-1H-pyrrole (0.3004 g, 1.370 mmol), trimethylbenzoic acid (0.1333 g, 8.118 mmol), and phosphorous oxychloride (5.0 mL, 0.54 mmols) were added. The

mixture was heated to 95 °C and stirred for 1 hour. A dark tar like product formed in solution and the mixture was poured over ice (~100 mL) and sat for 10 minutes, quenching any unreacted phosphorous oxychloride. The mixture was then brought to boil with stirring, the tar-like product dissolving into a murky brown suspension. The product, appearing as a grainy, gray solid, was then separated by decantation.

The gray solid was dissolved in methanol (MeOH, 75 mL). The solution was poured into 100 mL of 0.1 M NaOH, resulting in the formation of peach-colored precipitate. The product was separated by vacuum filtration and washed 3 times with water, resulting in a clay-like solid. The solid was dissolved in isopropanol and filtered. The solvent was removed under reduced pressure. NMR analysis was done using deuterated chloroform ($CDCl_3$) as the solvent. Upon dryness, the product presented itself as a green solid.

Synthesis of *bis*(1,3,7,9-tetraphenyl-5-mesityldyrronato) zinc(II):

This synthesis was based on literature method described by the Thompson Lab[25]. Without further purification, MeOH (13.2 mL) and triethyl amine (TEA, 0.0726 mL) were added to the ligand. In a separate container, zinc acetate (0.233 g, 1.27 mmol) was dissolved in methanol (3.3 mL) and mixtures were combined, forming a deep red coloration. The mixture was left to stir overnight. No solid precipitate formed, and the solvent was removed under reduced pressure to result in a dark red oil. The oil was dissolved in 15 mL chloroform and washed three times with a similar volume of 0.1 M HCl and once with a similar volume of water. The organic layer was separated, and the solvent was removed under reduced pressure to produce a deep green-brown solid. NMR analysis was conducted in $CDCl_3$.

Attempt 2:

This synthesis was repeated using 0.3051 g (1.391 mmol) 2,4-diphenyl-1H-pyrrole and 0.1298 g (0.7905 mmol) trimethylbenzoic acid to similar results for the ligand synthesis step. An attempt to purify the muddy, peach-colored solid was made by dissolution in hot methanol and the addition of water to form a precipitate. The light brown precipitate was dried in a desiccator for 1 ½ hours before NMR analysis was performed with $CDCl_3$ as the solvent. There was no solid product from the zinc coordination and the solvent was removed under reduced pressure, resulting in a dark red, oily solid. Purification steps were attempted, but the organic layer was spilled preventing analysis via NMR.
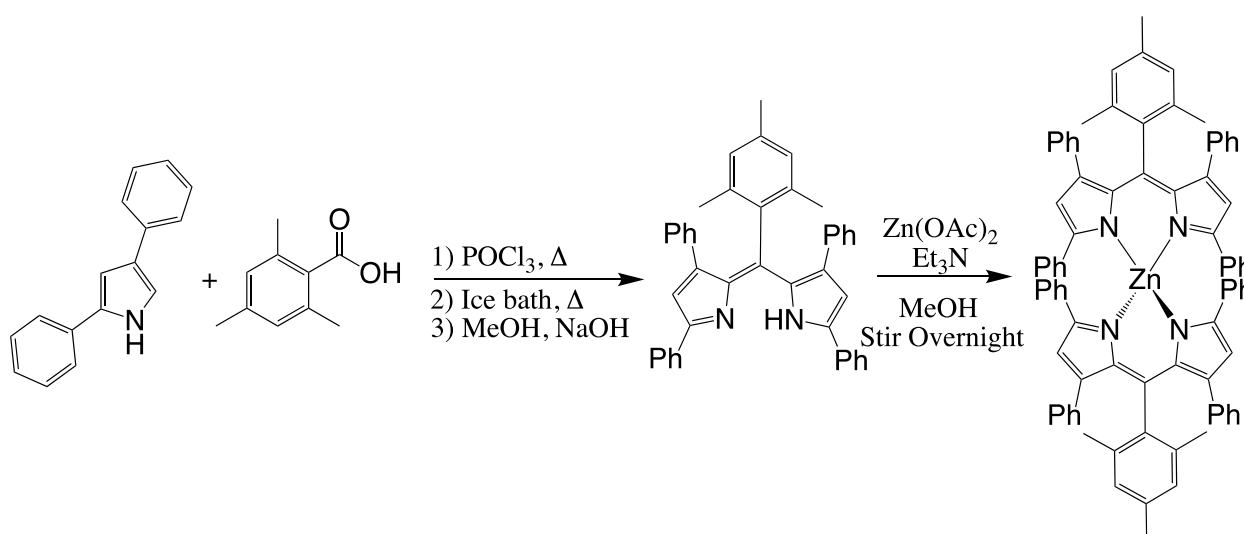
Synthesis B
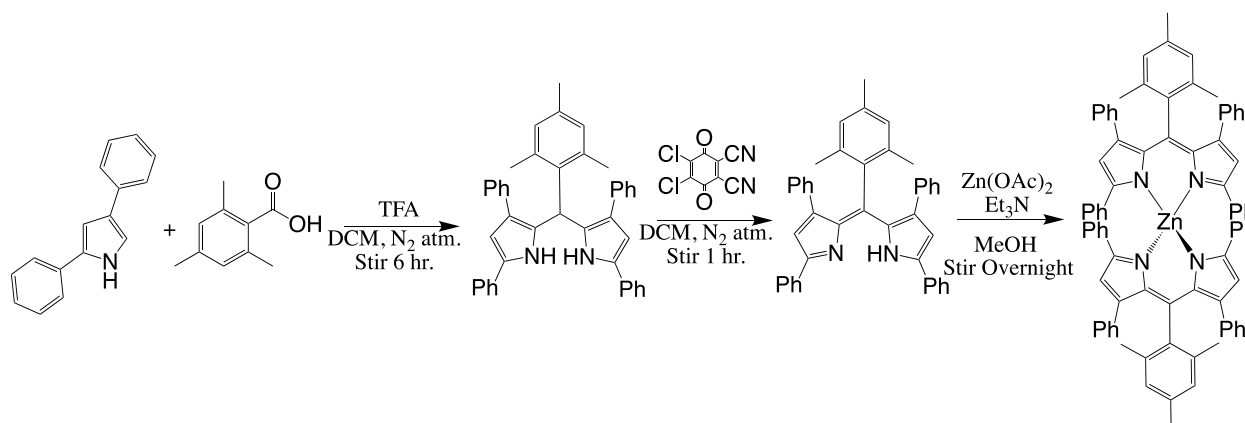
Figure 13: The synthesis B reaction scheme.

Attempt 1:

Synthesis of 1,3,7,9-tetraphenyl-mesityldipyrromethane:

All steps of synthesis B are based on literature method described by the Thompson Lab[25], with modification regarding the starting pyrrole. To 20 mL of DCM, 2,4-diphyenyl-1H-pyrrole (0.2510 g, 1.145 mmol) and mesitaldehyde (0.23 g, 1.552 mmol) were added under a nitrogen atmosphere. Once dissolved, 3 drops of

trifluoroacetic acid (TFA) was added and the mixture was stirred under nitrogen for 6 hr, darkening in color over the course of the reaction. To quench the reaction, 3 drops of TEA were added, inducing a color change to light orange and production of an opaque gas. The reaction mixture was washed once with 0.1M HNO_3, 3 times with water and once with brine. The organic layer was collected and allowed to evaporate. The product, a silvery-green solid assumed to be composed of some of the desired dipyrromethane, was used in the next step without intermediate purification.

Aromatization to 1,3,7,9-tetraphenyl-5-mesityldiprromethene:

To the ligand, 10 mL of freshly distilled THF was added under a nitrogen atmosphere. 2,3-Dichloro-5,6-dicyano-1,4-benzoquinone or DDQ (0.3500 g, 3.238 mmol) was dissolved in 4.5 mL of THF and then added to the reaction mixture, inducing a color change to a dark blue green. To this, 0.5 mL of TEA was added, inducing a color change to deep red. The solvent was removed under reduced pressure and an oily product was left over. This solid was dissolved in ~20 mL of DCM and the organic layer was washed three times with 0.1M HNO_3, once with water, and once with brine. The organic layer was separated, and the solvent was removed under reduced pressure. The resulting coppery green oil was dissolved in CDCl3, and an NMR spectrum was taken. The product was assumed to be the desired dipyrrin ligand (0.22 g) and was used in the following step without intermediate purification.

Synthesis of *bis*(1,3,7,9-tetraphenyl-5-mesityldipyrronato) zinc(II):

The dipyrrin was dissolved in 13.3 mL of MeOH, followed by 0.0726 mL of triethylamine. Zinc acetate dihydrate (0.236 g, 1.075 mmol) was dissolved in 3.3 mL of MeOH and was added to the reaction mixture and the solution was left to stir overnight. The solvent was removed under reduced pressure, yielding a red oil. This product was

dissolved in ~40 mL of DCM and washed 3 times with 0.1M HCl and once with water. The organic layer was separated, and the solvent was removed under reduced pressure. The resulting coppery green oil was dissolved in DCM and passed through a 2" alumina plug. The solvent was removed from the filtrate under reduced pressure, yielding a purple oil, which was dried in a desiccator. The product was passed through a 6" silica gel column using 10:90 ethyl acetate to hexanes as the eluent. In 5 mL intervals, 19 pink colored fractions were collected. TLC was performed on these fractions to determine which were of similar identity, those fractions being combined. The combined fractions were left to dry, dissolved in deuterated dimethyl sulfoxide (DMSO), and analyzed via NMR spectroscopy.

Attempt 2:

In DCM, 2,4-diphenyl-1H-pyrrole (2.500 g, 11.40 mmol) reacted with mesitaldehyde (0.8510g, 5.742 mmol). The dipyromethane and dipyrromethane synthesis were performed similarly as described above. The coordination of the dipyrrin to zinc was accomplished with an excess of zinc acetate (1.903 g, 8.671 mmol). The product was dissolved in hexanes and filtered. The filtrate evaporated, yielding a deep purple solid, and a residue was isolated. These components were dissolved in $CDCl_3$ and analyzed via NMR. The purple component was passed through a 6" alumina column using 20:80 hexanes to toluene as the solvent. Fractions were collected, analyzed by TLC, and like fractions were combined. The combined fractions were allowed to evaporate and dry and were dissolved in $CDCl_3$ for NMR analysis. Fraction 1-3 resulted in a spectrum most akin to expected product, and this fraction was dissolved in hexanes for analysis via UV-Vis spectroscopy between 300 and 800 nm.

Attempt 3:

2,4-diphenyl-1H-pyrrole (0.5010 g, 2.285 mmols) was reacted with mesitaldehyde (0.170 g, 1.147 mmol) as prior, but the reaction was allowed to run 58 hours while monitoring with TLC using 10:90 ethyl acetate to hexanes as the eluent. The resulting dipyrromethane was aromatized and coordinated to zinc according to the previous methodology with stoichiometric amounts of reagents. The intermediate and final products were analyzed by NMR in $CDCl_3$. The synthesis resulted a deep purple product of low yield.

Chapter 3: Results and Discussion

Synthesis A:

In both attempts, synthesis A yielded a dipyrrin product that was initially of a clay brown coloration (Figure 14). This is an immediate indication that the reaction failed to progress as planned with any decent yield. The aromatized dipyrrin should strongly absorb visible light, its predecessors being of green, yellow, and red colorations[10,19]. NMR analysis showed a very crowded aromatic region, confounded by the persistence of starting pyrrole in the system.

Figure 14: The solid precipitate following the addition of NaOH to the MeOH solution in the synthesis A. This step yields the dipyrrin, which should be very active in the visible region.

Two broad peaks at δ = 8.717 and 8.447 ppm may be indicative of N-H bond signals, either from the dipyrromethene or the starting pyrrole. A peak at δ = 9.877 ppm may be indicative of the O-H bond of trimethylbenzoic acid, although it is much further upfield than previously reported[55]. Ideally, there is a signal corresponding to the pyrrolic C-H hydrogen at δ ≅ 5.9 ppm[18] (Figure 15). There is no such peak in this spectrum. It appears that some alteration of the starting materials has occurred, but not that of the

desired results. It is appropriate to note that the NMR spectra are generally

unintelligible, which may be due to issues in functionality in the NMR spectrometer at

the time of this synthesis.
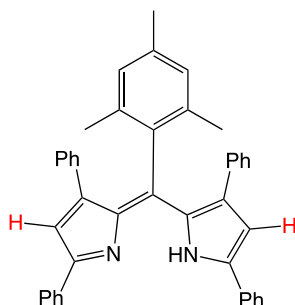
Figure 15: The pyrrolic hydrogens of 1,3,7,9-tetraphenyl-5-mesityldipyrromethene.
Phenyl groups are abbreviated 'Ph'.

The zinc coordination step of Synthesis A yielded a very small amount of a

greenish-brown solid. The NMR analysis provided no confirmation of the ZnDIPY

present in the system. The addition of the zinc central atom eliminates the N-H bond of

the dipyrrin ligand, and the most noticeable change in the chemical environments of the

hydrogens in the structure would occur at the pyrrolic hydrogens, as these are closest to

the coordination site (Figure 16). This change should alter the chemical shifts of these

hydrogens to some degree when compared to the free ligand. A persistence of the

pyrrolic N-H signal at ~9.8 ppm indicates that this synthesis had little success, and

there was no identification of a shift in the pyrrolic hydrogen signals.
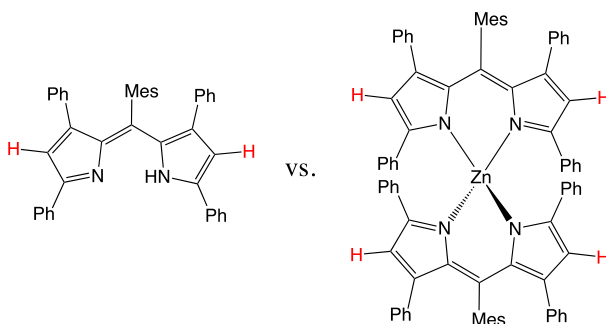
Figure 16: The pyrrolic hydrogens of the dipyrromethene vs. the ZnDIPY. Phenyl and
mesityl ('Mes') groups are abbreviated.

Synthesis B:

The dipyrromethane step of synthesis B yielded a brownish-green, flaky solid, much like the starting pyrrole. This synthesis results in the unconjugated form of the dipyrrin, meaning the conjugated pi chain does not expand and the absorption and emission qualities are not expected to change. Ideally, a singlet peak representing the C-H bond of the methylene bridge would be present at $\delta \cong 5.7$ ppm [19] (Figure 17). There is no such peak in the spectrum.
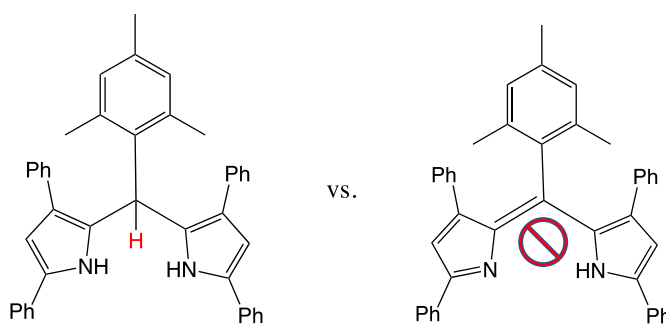
Figure 17: The unsaturation of the methylene bridge from dipyrromethane to dipyrromethene.

A singlet at 6.241 ppm may be indicative of a pyrrolic C-H signal on the dipyrromethane. Methyl ($-CH_3$) signals of the dipyrromethane shifted upfield from those of the starting mesitaldehyde to 2.215 ppm and 2.018 ppm, with integration values of ~1:2 as expected. The ratios of mesitaldehyde $-CH_3$ peaks to dipyrromethane $-CH_3$ peaks are 2.72 for the ortho-positioned methyl groups and 3.04 for the para-positioned methyl groups (Figure 18).
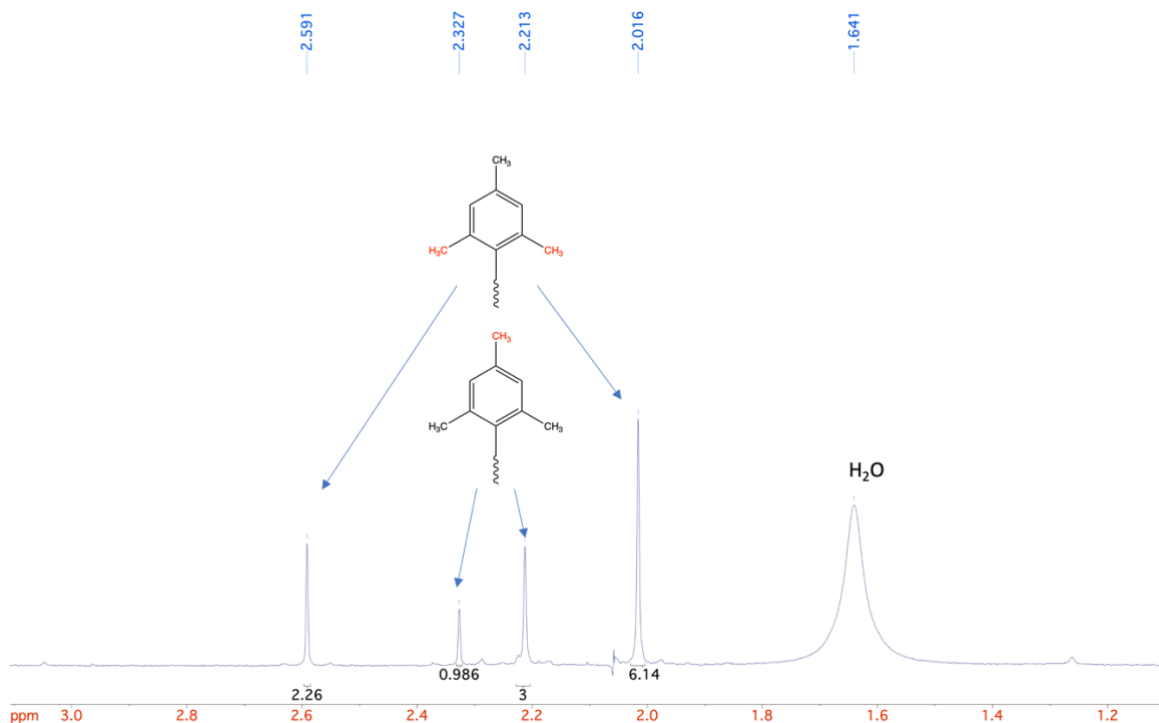
Figure 18: Methyl signals in the ¹H NMR of the dipyrromethane product of Synthesis B, attempt 2. The upfield signals are of the dipyrromethane, whereas the downfield signals are of the starting mesitaldehyde.

The aromatic region has high activity, with a multiplets and doublets ranging from ~7.10 ppm to ~7.60 ppm, integrating to values in the multiple hundreds. This is much higher than expected for the dipyrrin structure, and these inflated values are likely caused by aromatic hydrogens present in the unreacted starting pyrrole. A new broad peak presents itself at 8.084 ppm, indicating the pyrrolic N-H bond present in the dipyrrin structure. The peaks indicative of the starting materials are still prevalent in the dipyrromethane, meaning the reaction did not reach completion in 6 hours, opposing previous syntheses which reported quantitative yields in this step[10,19,25]. This is most likely due to the bulky phenyl substitutions on the starting pyrrole inhibiting the interaction with the other reagents, as it is well established that steric hindrance often has a retarding effect on reaction rate[56]. It must also be noted that this reaction is

occurring at much lower concentrations than those from the source literature, as the mass of the phenyl substituted pyrrole is greater than the starting pyrroles used in the source.

Upon the addition of the DDQ oxidizing agent, the coordination of the two pyrrole rings through the methylene bridge elongates the pi system and induced a color change to a very dark green. It is worth mentioning that the color qualities of this molecule are extremely flexible, appearing coppery green in acidic solution and a dark red in basic solutions, a characteristic observed in similar dipyrrin structures that may be induced by the protonation state of the pyrrolic hydrogen[20]. NMR analysis of the product reveals the continued presence of starting materials and solvent peaks, and little perceived change from the spectrum of the dipyrromethane form. This is expected, since the only major change is the loss of the C-H singlet of the methylene bridge in its conversion to the methine bridge form (Figure 17). Since this peak was never identified in the dipyrromethene, there is no indication of change, other than slight shifts in some signals.

Synthesis the bis(1,3,7,9-5-mesityl-dipyrronato)zinc(II) compound resulted in extremely low yields of a purple solid. No precipitate formed from the coordination of zinc to the dipyrrin ligand, which opposes previous synthesis procedures of like molecules[57,58]. The bulkiness of the phenyl groups on the ZnDIPY may alter its solubility in methanol. Since the reaction relies on the precipitation of the product to induce a shift further towards the products by Le Chatelier's principle, this may be a variable which reduces yield in the step. To remedy this, a synthesis was attempted with excess zinc acetate to artificially force the reaction equilibrium towards the product.
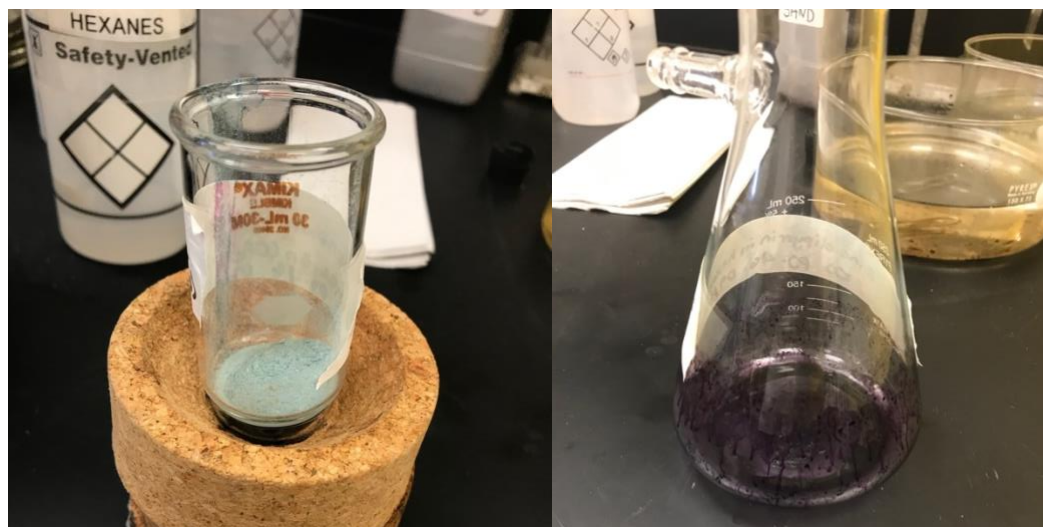
Figure 19: The light blue residue (left) of the hexanes extraction of the product of the bis(1,3,7,9-5-mesityl-dipyrronato)zinc(II) synthesis, and the deep purple solid (right) produced from the filtrate.

It is unclear if additional zinc acetate improved yield. However, solubility tests indicated the presence of an insoluble residue in hexanes. A hexanes extraction yielded a light blue residue, and a deep purple filtrate (Figure 19). NMR analysis was done before and after the extraction, revealing the light blue product as unreacted pyrrole. The purple product may be confirmed as the desired product (Figure 20, Table 1). It retained the methyl groups of the mesityl substituents, as well as the pyrrolic C-H signal expected in the desired structure. A slight upfield shift occurred in the pyrrolic C-H signal, from 6.232 ppm to 6.228 ppm, potentially caused by a change in the chemical environment induced by the coordination of zinc.
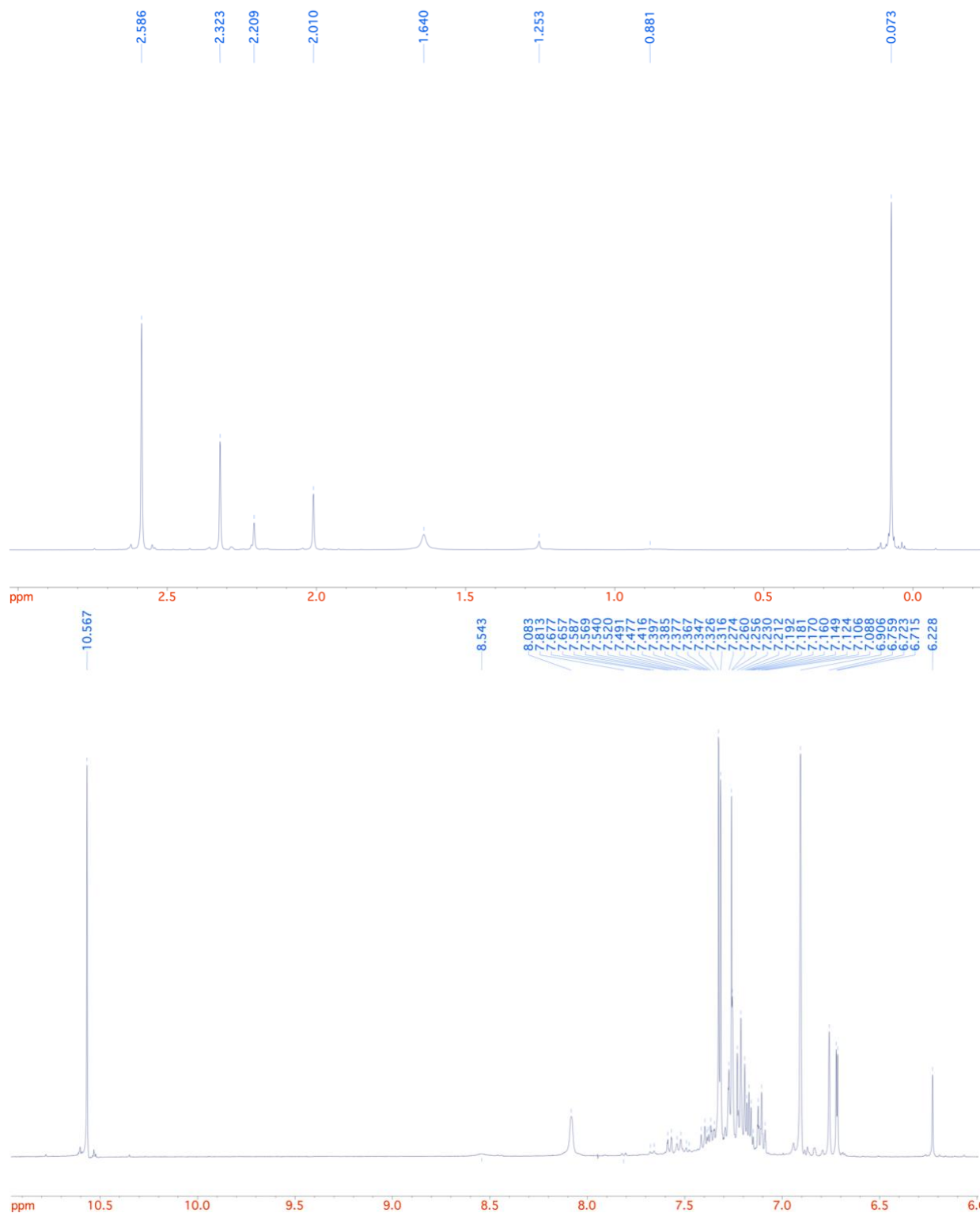
Figure 20: NMR of bis(1,3,7,9-5-mesityl-dipyrronato)zinc(II) synthesis succeeding hexanes extraction from 0.0 ppm to 3.0 ppm (top) and from 6.0 to 10.6 ppm (bottom). See Table 1 in Appendix A for integration and interpretation.

The ZnDIPY product was run through an alumina column, separating the product into a pink band that eluted quickly and a red band that persisted on top of the alumina. The red band is uncoordinated dipyrrin whose nitrogen cling to the alumia[18]. The silica column separated colored bands throughout its length (Figure 21, left). A bright purple-pink band, the most visibly active passed through the column first, then a lighter pink band, and finally by a UV active component with very light pink coloration (Figure 21, right). Some bands remained in the column despite the amount of eluent passed through the column. Fractions 1-3 yielded a deep pink-purple solid and were consolidated, fractions 4-6 yielded an emerald-green solid and were consolidated, fractions 7 and 8 yielded a small amount of purple solid and were consolidated, and fractions 9-12 were highly UV active and yielded very small amount of light purple solid of elongated crystals. Fractions 2, 5, 7 and 8 together, and 10 analyzed by NMR in CDCl$_3$, revealing that fractions 1-3 are most likely the desired products. The mesitaldehyde CH$_3$ peaks were removed from the spectrum, and the aromatic region integrates to a much lower value, indicating an increase in purity and removal of most of the starting materials. Fractions 4-8 are composed predominantly of mesitaldehyde starting material and some trace pyrrole and ZnDIPY, and fraction 10 was composed of the starting pyrrole.

Figure 21: The silica column used to separate the ZnDIPY from the other components of the reaction mixture (left), and the example of a fraction, fraction 10, which was highly UV active (right).

The product of fractions 1-3 were further analyzed via UV-Vis spectroscopy. Previous analysis of these compounds shows that the absorbance peaks are sharp and Gaussian in nature[10,17,25]. The absorption spectra of this compound indicate a maximum between 520 and 545 nm (Figure 22). The spectrum reveals a shoulder near the peak of the curve, indicating some sort of impurity that broadens the peak. Thus, the chromatography step did not accomplish complete purification, and further steps are required. The yield of this synthesis attempt was too low to initiate further purification steps, and was very low overall, although not quantified.
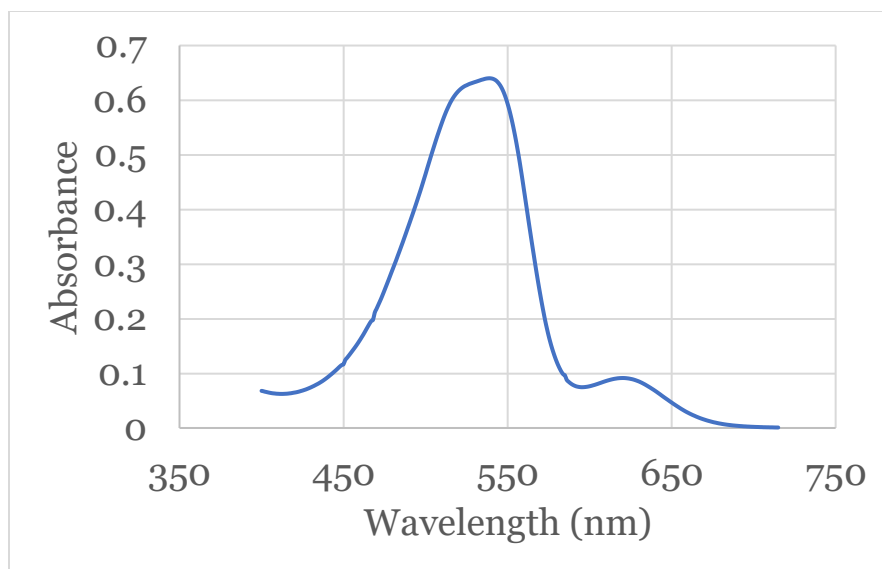
Figure 22: The absorbance spectrum of the ZnDIPY product in fractions 1-3.

The low yield was hypothesized to originate in part in the dipyrromethene synthesis step due to the bulky phenyl groups of the starting pyrrole, and allowing the reaction to run longer was attempted to increase overall yield. The synthesis was carried out to the zinc coordination, and this attempt also resulted in a deep purple solid. NMR analysis shows impuriy in the final product, so yield cannot be calculated. TLC monitorring of the dipyrromethane synthesis step indicated 3 components in the reaction mixture throughout the reaction: the starting mesitaldehyde, pyrrole, and the dipyrromethane product. Over the course of the reaction, TLC indicated that the product increased in concentration, but with maintained prelevence of the starting materials. NMR analysis of the dipyrromethane product indicates ratios of product to starting mesitaldehyde -CH_3 peaks of are 2.40 for the para-positioned methyl groups and 2.30 for the ortho-positioned methyl groups (Figure 23). This indicates that the extended reaction time did little to increase dipyrromethane yields, since both attempt 2

and 3 utilized stoichiometric equivlents of the starting mesitaldehyde and pyrrole and

attempt 2 produced greater product to starting material ratios in the NMR analysis.

Figure 23: Methyl signals in the ¹H NMR of the dipyrromathane product of Synthesis B, attempt 3. The upfield signals are of the dipyrromethane, whereas the downfield signals are of the starting mesitaldehyde.
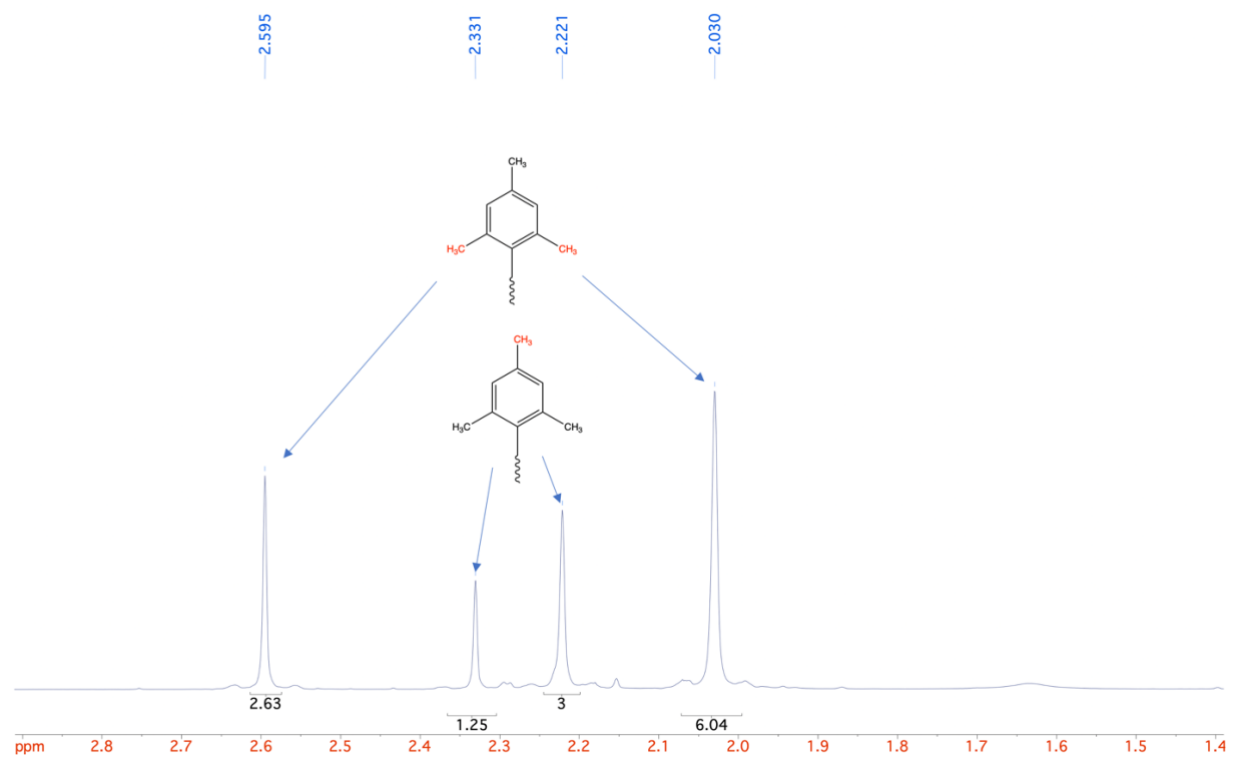
Chapter 4: Conclusions

In this experiment, synthesis of bis(1,3,7,9-tetraphenyl-5-mesityldipyrronato) zinc(II) was attempted using two literature methods to probe the effect of aromatic substitution on the photochemical and photophysical characteristics of the zinc dipyrrin class of photosensitizers.

The first was the reaction was of 2,4-diphenyl-1H-pyrrole with trimethylbenzoic acid catalyzed by phosphorous oxychloride, and the second was the reaction of pyrrole with an aldehyde catalyzed by trifluoroacetic acid, both followed by the coordination to zinc using zinc acetate. The former method failed to synthesize the desired product, whereas the later method yielded good evidence that the product was successfully synthesized, albeit with low yields. An extended reaction time in the dipyrromethane synthesis step of the latter method failed to increase the reaction yield of this step, and quantitative yields like those reported in like syntheses[17,25] were far from achieved. Low yields prevented purification without loss of most of the product, so further structural characterizations like high resolution mass spectroscopy and elemental analysis were not accomplished. Future experiments may include scaling up the synthesis to isolate enough product for sufficient purification, with final yields high enough to quantify the photophysical characteristics of the compound. These photophysical characterizations include reporting absorption and emission spectral data, the molar absorptivity, and the triplet state yield in solvents of various polarities.

Coordination of the ligand to zinc before purification allowed the product to elute with good efficiency, as opposed to the inefficient separation reported Meredith's thesis[18], resolving the perceived issue. The results of this experiment pose two new problems: 1) how is the dipyrromethane step yield further increased and 2) what solvent

system may result in the precipitation of the phenyl substituted ZnDIPY in the zinc coordination step? An obvious remedy may be to increase the concentration of the starting materials in the synthesis of dipyrromethane. Another potential optimization in methodology is to consider size exclusion chromatography to separate the dipyrrin ligand from ZnDIPY.

Future aims of this research are to characterize the bis(1,3,7,9-tetraphenyl-5-mesityldipyrronato) zinc(II) in its pure form and quantify its photophysical characteristics as previously mentioned. Synthesis of a BoDIPY with the 1,3,7,9-tetraphenyl-5-mesityldipyrrin ligand will be performed to compare the triplet state yield of the ZnDIPY and the BoDIPY in solvents of various polarities to probe the role of CS state formation in ISC within the ZnDIPY.

References

(1)   United States Environmental Protection Agency. *Global Greenhouse Gas Emissions Data* . https://www.epa.gov/ghgemissions/global-greenhouse-gas-emissions-data (accessed 2023-04-06).

(2)   Yoro, K. O.; Daramola, M. O. CO2 Emission Sources, Greenhouse Gases, and the Global Warming Effect. *Advances in Carbon Capture: Methods, Technologies and Applications* **2020**, 3–28. https://doi.org/10.1016/B978-0-12-819657-1.00001-3.

(3)   Bates, N. R.; Astor, Y. M.; Church, M. J.; Currie, K.; Dore, J. E.; González-Dávila, M.; Lorenzoni, L.; Muller-Karger, F.; Olafsson, J.; Santana-Casiano, J. M. A Time-Series View of Changing Surface Ocean Chemistry Due to Ocean Uptake of Anthropogenic CO2 and Ocean Acidification. *Oceanography* **2014**, *27* (1), 126–141. https://doi.org/10.5670/OCEANOG.2014.16.

(4)   Wolfram, P.; Lutsey, N. Electric Vehicles: Literature Review of Technology Costs and Carbon Emissions.

(5)   Zhang, B.; Sun, L. Artificial Photosynthesis: Opportunities and Challenges of Molecular Catalysts. *Chem Soc Rev* **2019**, *48* (7), 2216–2264. https://doi.org/10.1039/C8CS00897C.

(6)   Dau, H.; Fujita, E.; Sun, L. Artificial Photosynthesis: Beyond Mimicking Nature. *ChemSusChem* **2017**, *10* (22), 4228–4235. https://doi.org/10.1002/CSSC.201702106.

(7)   Lawrence Livermore National Laboratory. *Energy Flow Charts*. https://flowcharts.llnl.gov/commodities/energy (accessed 2023-02-23).

(8)   Eneh; Onyenekenwa C. A Review on Petroleum: Source, Uses, Products, and the Environment. *Journal of Applied Sciences* **2011**, *11* (12), 2084–2091.

(9)   International Energy Agency. *Petrochemicals Set to Be the Largest Driver of World Oil Demand, Latest IEA Analysis Finds* ; 2018. https://www.iea.org/news/petrochemicals-set-to-be-the-largest-driver-of-world-oil-demand-latest-iea-analysis-finds (accessed 2023-03-01).

(10)   Alqahtani, N. Synthesis and Characterization of Zinc(II) Dipyrrin Photosensitizers, 2018. https://dc.etsu.edu/etd/3466.

(11)   Witzel, S.; Stephen, A.; Hashmi, K.; Xie, J. Light in Gold Catalysis. **2021**. https://doi.org/10.1021/acs.chemrev.0c00841.

(12)   Koike, T.; Akita, M. Visible-Light Radical Reaction Designed by Ru- and Ir-Based Photoredox Catalysis. *Inorg Chem Front* **2014**, *1* (8), 562–576. https://doi.org/10.1039/c4qi00053f.

(13)   Dhakshinamoorthy, A.; Asiri, A. M.; García, H. Metal–Organic Framework (MOF) Compounds: Photocatalysts for Redox Reactions and Solar Fuel Production. *Angewandte Chemie International Edition* **2016**, *55* (18), 5414–5445. https://doi.org/10.1002/ANIE.201505581.

(14)   Shirley, H.; Su, X.; Sanjanwala, H.; Talukdar, K.; Jurss, J. W.; Delcamp, J. H. Durable Solar-Powered Systems with Ni-Catalysts for Conversion of CO2 or CO to CH4. *J Am Chem Soc* **2019**, *141* (16), 6617–6622. https://doi.org/10.1021/jacs.9b00937.

(15)   Sabatini, R. P.; Lindley, B.; McCormick, T. M.; Lazarides, T.; Brennessel, W. W.; McCamant, D. W.; Eisenberg, R. Efficient Bimolecular Mechanism of Photochemical Hydrogen Production Using Halogenated Boron-Dipyrromethene (Bodipy) Dyes and a Bis(Dimethylglyoxime) Cobalt(III) Complex. *Journal of Physical Chemistry B* **2016**, *120* (3), 527–534. https://doi.org/10.1021/acs.jpcb.5b11035.

(16) Lutkus, L. *Applications of Triplet-Photosensitizers and Development of Photochemical Methods*; Portland, OR, 2020. https://doi.org/10.15760/etd.7290.

(17) Alqahtani, N. Z.; Blevins, T. G.; McCusker, C. E. Quantifying Triplet State Formation in Zinc Dipyrrin Complexes. *Journal of Physical Chemistry A* **2019**. https://doi.org/10.1021/acs.jpca.9b08682.

(18) Meredith, S. Synthesis of a Zinc Dipyrrin Complex for Photocatalytic Reduction Synthesis of a Zinc Dipyrrin Complex for Photocatalytic Reduction of CO2 of CO2, 2021. https://dc.etsu.edu/honors/645.

(19) Dzaye, I. Y. Investigating the Role of Charge Separation in Triplet State Investigating the Role of Charge Separation in Triplet State Formation in Zinc Dipyrrin Photosensitizers, 2021. https://dc.etsu.edu/etd/3912.

(20) Taşkıran, Z. P.; Sevinç, G. Photophysical Characterization of Novel Dipyrrine Compounds Based on Pyrrolic Hydrogen Transfer. *J Mol Struct* **2022**, *1260*. https://doi.org/10.1016/j.molstruc.2022.132794.

(21) Li, J.; Hu, B.; Hu, G.; Li, X.; Lu, P.; Wang, Y. An Efficient Synthesis of Heptaaryldipyrromethenes from Tetraarylcyclopentadienones and Ammonium Acetate and Their Extension to the Corresponding BODIPYs. *Org Biomol Chem* **2012**, *10* (44), 8848–8859. https://doi.org/10.1039/c2ob26509e.

(22) Tsuchiya, M.; Sakamoto, R.; Kusaka, S.; Kakinuma, J.; Nishihara, H. Triarylamine-Conjugated Bis(Dipyrrinato)Zinc(II) Complexes: Impact of Triarylamine on Photochemical Property and Multi-Redox Reaction. *Electrochemistry* **2013**, *81* (5), 337–339. https://doi.org/10.5796/electrochemistry.81.337.

(23) Kusaka, S.; Sakamoto, R.; Kitagawa, Y.; Okumura, M.; Nishihara, H. An Extremely Bright Heteroleptic Bis(Dipyrrronato)Zinc(II) Complex. *Chemistry: An Asian Journal* **2012**, *7*, 907–910.

(24) Kee, H. L.; Kirmaiery, C.; Yu, L.; Thamyongkit, P.; Youngblood, W. J.; Calder, M. E.; Ramos, L.; Noll, B. C.; Bocian, D. F.; Scheldt, W. R.; Birge, R. R.; Lindsey, J. S.; Holten, D. Structural Control of the Photodynamics of Boron-Dipyrrin Complexes. *Journal of Physical Chemistry B* **2005**, *109* (43), 20433–20443. https://doi.org/10.1021/jp0525078.

(25) Trinh, C.; Kirlikovali, K.; Das, S.; Ener, M. E.; Gray, H. B.; Djurovich, P.; Bradforth, S. E.; Thompson, M. E. Symmetry-Breaking Charge Transfer of Visible Light Absorbing Systems: Zinc Dipyrrins. *Journal of Physical Chemistry C* **2014**, *118* (38), 21834–21845. https://doi.org/10.1021/jp506855t.

(26) Tao, J.; Sun, D.; Sun, L.; Li, Z.; Fu, B.; Liu, J.; Zhang, L.; Wang, S.; Fang, Y.; Xu, H. Tuning the Photo-Physical Properties of BODIPY Dyes: Effects of 1, 3, 5, 7- Substitution on Their Optical and Electrochemical Behaviours. *Dyes and Pigments* **2019**, *168*, 166–174. https://doi.org/10.1016/j.dyepig.2019.04.054.

(27) Tsuchiya, M.; Sakamoto, R.; Shimada, M.; Yamanoi, Y.; Hattori, Y.; Sugimoto, K.; Nishibori, E.; Nishihara, H. Bis(Dipyrrinato)Zinc(II) Complexes: Emission in the Solid State. *Inorg Chem* **2016**, *55* (12), 5732–5734. https://doi.org/10.1021/acs.inorgchem.6b00431.

(28) Sazanovich, I. v; Kirmaier, C.; Hindin, E.; Yu, L.; Bocian, D. F.; Lindsey, J. S.; Holten, D. Structural Control of the Excited-State Dynamics of Bis(Dipyrrinato)Zinc Complexes: Self-Assembling Chromophores for Light-Harvesting Architectures. *J. AM. CHEM. SOC* **2004**, *126*, 2664–2665. https://doi.org/10.1021/ja038763k.

(29) NREL. *Reference Air Mass 1.5 Spectra* . https://www.nrel.gov/grid/solar-resource/spectra-am1.5.html (accessed 2023-02-20).

(30) Fleischer, M. THE ABUNDANCE AND DISTRIBUTION OF THE CHEMICAL ELEMENTS IN THE EARTH'S CRUST. *J. Chem. Edu* **1954**, *31* (9), 446–455.

(31) Pellegrin, Y.; Odobel, F. Sacrificial Electron Donor Reagents for Solar Fuel Production. *Comptes Rendus Chimie* **2017**, *20* (3), 283–295. https://doi.org/10.1016/J.CRCI.2015.11.026.

(32) Revol, G.; Mccallum, T.; Morin, M.; Gagosz, F.; Barriault, L. Photoredox Transformations with Dimeric Gold Complexes. *Angewandte Chemie* **2013**, *125* (50), 13584–13587. https://doi.org/10.1002/ange.201306727.

(33) Siu, C. H.; Lee, L. T. L.; Yiu, S. C.; Ho, P. Y.; Zhou, P.; Ho, C. L.; Chen, T.; Liu, J.; Han, K.; Wong, W. Y. Synthesis and Characterization of Phenothiazine-Based Platinum(II)-Acetylide Photosensitizers for Efficient Dye-Sensitized Solar Cells. *Chemistry* **2016**, *22* (11), 3750–3757. https://doi.org/10.1002/CHEM.201503828.

(34) Chemistry LibreTexts. *11.4: The Effect of the Metal Ion on d-Orbital Splitting* . https://chem.libretexts.org/Courses/Saint_Marys_College_Notre_Dame_IN/CHEM_431%3A_Inorganic_Chemistry_(Haas)/CHEM_431_Readings/11%3A_Ligand_Field_Theory_(LFT)_and_Crystal_Field_Theory_(CFT)_of_Octahedral_Complexes/11.04%3A_The_Effect_of_the_Metal_Ion_on_d-Orbital_Splitting (accessed 2023-04-08).

(35) Creutz, C.; Chou, M.; Netzel, T. L.; Okumura, M.; Sutin, N. Lifetimes, Spectra, and Quenching of the Excited States of Complexes of Iron(II), Ruthenium (II) and Osmium(II). *The Infra-Red Spectra of Complex Molecules* **1980**, *102* (4), 1309–1319.

(36) Chemistry LibreTexts. *Tanabe-Sugano Diagrams* . https://chem.libretexts.org/Ancillary_Materials/Reference/Reference_Tables/Spectroscopic_Reference_Tables/Tanabe-Sugano_Diagrams (accessed 2023-04-08).

(37) Fisher Scientific. *Zinc Acetate, Crystal, USP, 98-102%, Spectrum Chemical, Quantity: 100 g* . https://www.fishersci.com/shop/products/zinc-acetate-crystal-usp-98-102-spectrum-chemical-1/18607817?ef_id=Cj0KCQjwxMmhBhDJARIsANFGOSvs4cy-HsdstD8dh5s3G78CaiIxGkummnKKruX5RCQKRotY1auV-5UaAvHeEALw_wcB:G:s&ppc_id=PLA_HMD_goog_HighMargin_18631113532_147469056643_18607813__654254442683_12240935823826571446&ev_chn=shop&s_kwcid=AL!4428!3!654254442683!!!g!347500384935!18607813&gclid=Cj0KCQjwxMmhBhDJARIsANFGOSvs4cy-HsdstD8dh5s3G78CaiIxGkummnKKruX5RCQKRotY1auV-5UaAvHeEALw_wcB (accessed 2023-04-08).

(38) Fisher Scientific. *Ruthenium(III) chloride hydrate, 35 - 40% Ru, Thermo Scientific Chemicals, Quantity: 1 g* . https://www.fishersci.com/shop/products/ruthenium-iii-chloride-hydrate-35-40-ru-thermo-scientific/AC195480010 (accessed 2023-04-08).

(39) Fisher Scientific. *Iridium(III) chloride trihydrate, 53-56% Ir, Thermo Scientific Chemicals, Quantity: 1 g* . https://www.fishersci.com/shop/products/iridium-iii-chloride-trihydrate-53-56-ir-thermo-scientific/AC195500010 (accessed 2023-04-08).

(40) Lancashire, R. J. *Crystal Field Stabilization Energy* . Libretexts. https://chem.libretexts.org/Bookshelves/Inorganic_Chemistry/Supplemental_Modules_and_Websites_(Inorganic_Chemistry)/Crystal_Field_Theory/Crystal_Field_Stabilization_Energy (accessed 2023-03-31).

(41) Lancashire, R. J.; Awan, A.; Truong, H. *Crystal Field Theory* . Libretexts. https://chem.libretexts.org/Bookshelves/Inorganic_Chemistry/Supplemental_Modules_an

d_Websites_(Inorganic_Chemistry)/Crystal_Field_Theory/Crystal_Field_Theory (accessed 2023-03-31).

(42) Loudon, M.; Parise, J. *Organic Chemistry*, 6th ed.; W. H. Freeman : New York, 2016.

(43) Granger II, R. M. ; Y. H. M. ; G. J. N. ; S. K. D. *Instrumental Analysis*, 1st ed.; Oxford University Press: New York, 2017.

(44) Rasheed, S. Photocatalytic Carbon Dioxide Reduction with Zinc(II) Dipyrrin Photosensitizers and Iron Catalyst. Masters, East Tennessee State University, Johnson City, 2020. https://dc.etsu.edu/etd/3730.

(45) Tabero, A.; García-Garrido, F.; Prieto-Castañeda, A.; Palao, E.; Agarrabeitia, A. R.; García-Moreno, I.; Villanueva, A.; De La Moya, S.; Ortiz, M. J. BODIPYs Revealing Lipid Droplets as Valuable Targets for Photodynamic Theragnosis. *Chemical Communications* **2020**, *56* (6), 940–943. https://doi.org/10.1039/C9CC09397D.

(46) Pagano, R. E.; Chen, C. S. Use of BODIPY-Labeled Sphingolipids to Study Membrane Traffic along the Endocytic Pathwaya. *Ann N Y Acad Sci* **1998**, *845* (1), 152–160. https://doi.org/10.1111/J.1749-6632.1998.TB09668.X.

(47) Klfout, H.; Stewart, A.; Elkhalifa, M.; He, H. BODIPYs for Dye-Sensitized Solar Cells. *ACS Appl Mater Interfaces* **2017**, *9* (46), 39873–39889. https://doi.org/10.1021/ACSAMI.7B07688/ASSET/IMAGES/LARGE/AM-2017-07688D_0018.JPEG.

(48) García, O.; Sastre, R.; Del Agua, D.; Costela, A.; García-Moreno, I.; López Arbeloa, F.; Bañuelos Prieto, J.; López Arbeloa, I. Laser and Physical Properties of BODIPY Chromophores in New Fluorinated Polymeric Materials. *Journal of Physical Chemistry C* **2007**, *111* (3), 1508–1516. https://doi.org/10.1021/JP065080T/SUPPL_FILE/JP065080TSI20060807_102558.PDF.

(49) Loudet, A.; Burgess, K. BODIPY Dyes and Their Derivatives: Syntheses and Spectroscopic Properties. *Chem Rev* **2007**, *107* (11), 4891–4932. https://doi.org/10.1021/CR078381N/ASSET/CR078381N.FP.PNG_V03.

(50) Turksoy, A.; Yildiz, D.; Akkaya, E. U. Photosensitization and Controlled Photosensitization with BODIPY Dyes. *Coord Chem Rev* **2019**, *379*, 47–64. https://doi.org/10.1016/J.CCR.2017.09.029.

(51) Armarego, W. L. F.; Chai, C. L. L. *Purification of Laboratory Chemicals*, 7th ed.; Elsevier, Inc.: Oxford, 2009.

(52) Borys, A. M. An Illustrated Guide to Schlenk Line Techniques. *Organometallics* **2023**. https://doi.org/10.1021/acs.organomet.2c00535.

(53) Frontier, A. *Laboratory Techniques and Methods to Improve Your Experimental Skills*. https://www.chem.rochester.edu/notvoodoo/ (accessed 2023-02-05).

(54) Rogers, M. A. T. 157. 2 : 4-Diarylpyrroles. Part II. Methines. *Journal of the Chemical Society Resumed* **1943**, 596–597.

(55) Chemical BooK. *2,4,6-Trimethylbenzoic acid(480-63-7) 1H NMR spectrum*. https://www.chemicalbook.com/SpectrumEN_480-63-7_1HNMR.htm (accessed 2023-03-30).

(56) Liu, S.; Hu, H.; Pedersen, L. G. Steric, Quantum, and Electrostatic Effects on SN2 Reaction Barriers in Gas Phase. *J Phys Chem A* **2010**, *114* (18), 5913. https://doi.org/10.1021/JP101329F.

(57) Dudina, N. A.; Nikonova, A. Y.; Antina, Y. V; Berezin, M. B.; Vyugin, A. I. *SYNTHESIS, SPECTRAL-LUMINESCENT PROPERTIES, AND PHOTOSTABILITY OF Zn(II)*

COMPLEXES WITH DIPYRRINS MODIFIED BY THE PERIPHERY AND Meso-SPACER; 2014; Vol. 49.

(58)   Antina, E. V.; Berezin, M. B.; Dudina, N. A.; Burkova, S. L.; Nikonova, A. Y. Synthesis, Spectral-Luminescent Properties of B(III) and Zn(II) Complexes with Alkyl- and Aryl-Substituted Dipyrrins and Azadipyrrins. *Russian Journal of Inorganic Chemistry* **2014**, *59* (10), 1187–1194. https://doi.org/10.1134/S0036023614100027.

Appendix:

Table 1: The NMR spectrum of the purple product succeeding hexanes extraction.

Shift (δ)	Integration	Multiplicity	Identity
0.073	53	s	grease
0.881	1.846	m	hexanes
1.253	5.78	s	hexanes
1.64	14.78	s	water
2.01	12.08	s	o-methyl (product)
2.208	6	s	p-methyl (product)
2.323	20.8	s	p-methyl (mesitaldehyde)
2.586	41.8	s	o-methyl (mesitaldehyde)
6.228	1.97	s	pyrrolic C-H (product)
6.719	4.22	d	?
6.758	4.26	s	?
6.906	13.78	s	aromatic hydrogen (mesitaldehyde)
7.070 - 7.416	49.1	m	aromatic hydrogen (product)
7.477-7.813	1.21	m	aromatic hydrogen (diphenyl pyrrole)
7.812	0.238	dd	aromatic hydrogen (starting pyrrole)
8.083	3.8	bs	N-H (dipyrromethene)
8.54	0.728	bs	N-H (diphneyl pyrrole)
10.567	6.8	s	COH (mesitaldehyde)